Physics Letters B 751 (2015) 423–429

Contents lists available at ScienceDirect

Physics Letters B

www.elsevier.com/locate/physletb

Critical point symmetry for the spherical to triaxially deformed shape phase transition

Yu Zhang [a,*], Feng Pan [a,b], Yan-An Luo [c], J.P. Draayer [b]

[a] Department of Physics, Liaoning Normal University, Dalian 116029, PR China
[b] Department of Physics and Astronomy, Louisiana State University, Baton Rouge, LA 70803-4001, USA
[c] School of Physics, Nankai University, Tianjin 300071, PR China

ARTICLE INFO

Article history:
Received 18 September 2015
Received in revised form 15 October 2015
Accepted 28 October 2015
Available online 3 November 2015
Editor: J.-P. Blaizot

ABSTRACT

The critical point T(5) symmetry for the spherical to triaxially deformed shape phase transition is introduced from the Bohr Hamiltonian by approximately separating variables at a given γ deformation with $0° \le \gamma \le 30°$. The resulting spectral and $E2$ properties have been investigated in detail. The results indicate that the original X(5) and Z(5) critical point symmetries can be naturally realized within the T(5) model in the $\gamma = 0°$ and $\gamma = 30°$ limit, respectively, which thus provides a dynamical connection between the two symmetries. Comparison of the theoretical calculations for ^{148}Ce, ^{160}Yb, ^{192}Pt and ^{194}Pt with the corresponding experimental data is also made, which indicates that, to some extent, possible asymmetric deformation may be involved in these transitional nuclei.

1. Introduction

Critical point symmetries (CPSs) in nuclear structure have attracted a lot of attention [1–10], since these models may provide parameter-free (up to an overall scale) predictions about the structural properties of nuclei in the phase transitional region [11,12]. These CPSs include, for example, the critical point of the spherical to γ-unstable shape phase transition E(5) [1], the critical point of the spherical to axially deformed shape phase transition X(5) [2], and the critical point of the prolate to oblate shape phase transition Z(5) [4] (also serving as the CPS for the shape transition from the spherical to the triaxial deformation at $\gamma = 30°$), etc., which have been widely confirmed in experiment [13–20]. Generally, these CPS models are constructed from the Bohr Hamiltonian by separating the collective β and γ variables, and by making different assumptions about the potentials in β and γ. Specifically, separation of variables in the Bohr Hamiltonian for the X(5) model is achieved by assuming $\gamma = 0°$ [2], which represents an axially-symmetric situation, while that in the Z(5) model has been achieved by separating variables at $\gamma = 30°$ [4] corresponding to the maximally-triaxial situation. Moreover, in both models the potential in β is assumed to be an infinite square well, while the potential in γ is assumed to be a harmonic oscillator having a minimum at $\gamma = 0°$ for X(5) or $\gamma = 30°$ for Z(5).

The purpose of this work is to propose a Bohr Hamiltonian with a potential in γ having minimum at any given γ value with $\gamma \in [0°, 30°]$. The resulting model, which is called T(5), may provide a connection between the X(5) and Z(5) CPSs [2,4], which thus serves as the CPS for the transition from the spherical to a triaxial shape with $0° \le \gamma \le 30°$ since the X(5) and Z(5) symmetries can be used to describe the transitions from the spherical to axially deformed shape at $\gamma = 0°$ [2] and the spherical to triaxial-deformed shape at $\gamma = 30°$ [4], respectively. It should be mentioned that the spherical to triaxial-deformed shape phase transition can be alternatively analyzed within the interacting boson model [21] by introducing high-order terms in the Hamiltonian [22–25] since a rigid triaxial structure with a given γ deformation can principally be defined in such cases [24,25].

2. The model

The original Bohr Hamiltonian [26] is written as

$$H = -\frac{\hbar^2}{2B}\left\{\frac{1}{\beta^4}\frac{\partial}{\partial\beta}\beta^4\frac{\partial}{\partial\beta} + \frac{1}{\beta^2}\left(\frac{1}{\sin 3\gamma}\frac{\partial}{\partial\gamma}\sin 3\gamma\frac{\partial}{\partial\gamma} - \frac{1}{4}\sum_k \frac{L_k'^2}{\sin^2(\gamma - \frac{2}{3}k\pi)}\right)\right\} + V(\beta,\gamma), \quad (1)$$

* Corresponding author.
E-mail address: dlzhangyu_physics@163.com (Y. Zhang).

http://dx.doi.org/10.1016/j.physletb.2015.10.082

where β and γ are the deformation variables, B is the collective mass parameter, and L'_k $(k = 1, 2, 3)$ are the projections of the angular momentum on the body-fixed k-axis. In the present case, it is assumed [1–5] that

$$V(\beta,\gamma) = V(\beta) + V(\gamma), \tag{2}$$

in which the potential $V(\beta)$ is taken to be an infinite square well [2] with

$$V(\beta) = \begin{cases} 0, & \beta \le \beta_W, \\ \infty, & \beta > \beta_W, \end{cases} \tag{3}$$

whereas the potential $V(\gamma)$ is taken to be harmonic around $\gamma = \gamma_e$ [4] with

$$V(\gamma) = \frac{1}{2}C(\gamma - \gamma_e)^2. \tag{4}$$

As the potential has a minimum at $\gamma = \gamma_e$, the rotational term of Eq. (1) is approximated as

$$\begin{aligned} R_L &\equiv \sum_{k=1,2,3} \frac{L'^2_k}{\sin^2(\gamma - \frac{2}{3}k\pi)}\bigg|_{\gamma\simeq\gamma_e} \\ &= \frac{L'_1{}^2}{\sin^2(\gamma_e - \frac{2}{3}\pi)} + \frac{L'_2{}^2}{\sin^2(\gamma_e - \frac{4}{3}\pi)} + \frac{L'_3{}^2}{\sin^2(\gamma_e)}. \end{aligned} \tag{5}$$

Notably, the approximation used in (5) was also adopted in the X(5) and Z(5) models, but with $\gamma_e = 0°$ and $\gamma_e = 30°$ respectively. By introducing the reduced energy $\epsilon = 2BE/\hbar^2$ and reduced potentials $u = 2BV/\hbar^2$ [2,4], the corresponding Schrödinger equation can be separately written as

$$[-\frac{1}{\beta^4}\frac{\partial}{\partial\beta}\beta^4\frac{\partial}{\partial\beta} + \frac{r_L}{4\beta^2} + u(\beta)]\eta_L(\beta) = \epsilon_\beta \eta_L(\beta), \tag{6}$$

$$[-\frac{1}{\langle\beta^2\rangle \sin 3\gamma}\frac{\partial}{\partial\gamma}\sin 3\gamma\frac{\partial}{\partial\gamma} + u(\gamma)]\phi(\gamma) = \epsilon_\gamma \phi(\gamma), \tag{7}$$

where r_L is the eigenvalue of R_L, $\langle\beta^2\rangle$ is the average of β^2 over $\eta(\beta)$ [2], and $\epsilon = \epsilon_\beta + \epsilon_\gamma$. The total wave function can be constructed as

$$\Psi(\beta,\gamma,\theta_i) = \eta_L(\beta)\phi(\gamma)\varphi^L_{M,s}(\theta_i) \tag{8}$$

with

$$R_L\varphi^L_{M,s}(\theta_i) = r_{L_s}\varphi^L_{M,s}(\theta_i). \tag{9}$$

The rotational wave function $\varphi^L_{M,s}(\theta)$ can be expanded in terms of the Wigner D-functions with

$$\varphi^L_{M,s}(\theta_i) = \sum_K C^L_{s,K}\chi^L_{M,K}(\theta_i), \tag{10}$$

$$\begin{aligned}\chi^L_{M,K}(\theta_i) = &\sqrt{\frac{2L+1}{16\pi^2(1+\delta_{K,0})}} \\ &\times [D^L_{M,K}(\theta_i) + (-1)^L D^L_{M,-K}(\theta_i)], \end{aligned}\tag{11}$$

where $D^L_{M,K}(\theta_i)$ is the Wigner D-function, the expanding coefficients $C^L_{s,K}$ are determined from the eigenvalue equation (9), and s is used to label the s-th eigenstate for given L and M, which is given as

$$\begin{aligned} s &= 1,2,3,\ldots,\frac{L+2}{2}, \quad L = \text{even}, \\ s &= 1,2,3,\ldots,\frac{L-1}{2}, \quad L = \text{odd}. \end{aligned} \tag{12}$$

It should be noted that eigenvalue equation (9) can be analytically solved at $\gamma_e = 0°$ or $\gamma_e = 30°$, in which the values of r_L are respectively given as [2,4]

$$r_L(0°) = \frac{4}{3}[L(L+1) - K^2] + \frac{K^2}{\sin^2(\gamma_e)|_{\gamma_e\to 0°}} \tag{13}$$

and

$$r_L(30°) = 4L(L+1) - 3\alpha^2 \tag{14}$$

with α being the projection of the angular momentum on the body-fixed 1-axis. The resulting models just correspond to the X(5) and Z(5) CPSs, respectively. On the other hand, it should be noted that the last term $\frac{K^2}{\sin^2(\gamma_e)|_{\gamma_e\to 0°}}$ in (13) contributes nothing in the case of $K = 0$ [2] but an infinite number in the case of $K \ne 0$. To avoid such a situation, this term in the original X(5) model was absorbed into Eq. (7) [2]. Therefore, the $\gamma_e = 0$ situation shown in (13) only applies to the $K = 0$ case, while $K \ne 0$ cases have already been discussed in [2,27]. Generally, the r_L values, which are the eigenvalues of a triaxial rotor Hamiltonian, can only be numerically solved from (9) when $0° < \gamma_e < 30°$. But for a few of the lowest L values, r_{L_s} can be solved analytically from (9) as shown in [28,29], which are given as

$$r_{0_{s=1}}(\gamma_e) = 0, \tag{15}$$

$$r_{2_{s=1}}(\gamma_e) = \frac{18 - 6\sqrt{9 - 8\sin^2(3\gamma_e)}}{\sin^2(3\gamma_e)}, \tag{16}$$

$$r_{2_{s=2}}(\gamma_e) = \frac{18 + 6\sqrt{9 - 8\sin^2(3\gamma_e)}}{\sin^2(3\gamma_e)}, \tag{17}$$

$$r_{3_{s=1}}(\gamma_e) = \frac{36}{\sin^2(3\gamma_e)}, \tag{18}$$

$$r_{5_{s=1}}(\gamma_e) = \frac{90 - 18\sqrt{9 - 8\sin^2(3\gamma_e)}}{\sin^2(3\gamma_e)}, \tag{19}$$

$$r_{5_{s=2}}(\gamma_e) = \frac{90 + 18\sqrt{9 - 8\sin^2(3\gamma_e)}}{\sin^2(3\gamma_e)}. \tag{20}$$

Substituting $F(\beta) = \beta^{3/2}\eta(\beta)$ and $z = \beta k_\beta$ with $k_\beta = \sqrt{\epsilon_\beta}$ [2,4], one can transform Eq. (6) inside the well into the Bessel equation

$$\frac{d^2F}{dz^2} + \frac{1}{z}\frac{dF}{dz} + [1 - \frac{v^2}{z^2}]F = 0 \tag{21}$$

with

$$v = \sqrt{\frac{r_L + 9}{4}}. \tag{22}$$

Then the boundary condition $\eta(\beta_W) = 0$ determines the eigenvalues

$$\epsilon_{\beta;\,\xi,s,L} = (k_{\xi,v})^2, \quad k_{\xi,v} = (\frac{x_{\xi,v}}{\beta_W}), \tag{23}$$

and the eigenfunction

$$\eta_{\xi,s,L}(\beta) = c_{\xi,v}\beta^{-3/2}J_v(k_{\xi,v}\beta), \tag{24}$$

where $x_{\xi,v}$ is the ξ-th zero of the Bessel function $J_v(z)$, and the normalization constants $c_{\xi,v}$ are determined by

$$\int_0^\infty \beta^4\eta^2_{\xi,s,L}(\beta)d\beta = 1. \tag{25}$$

For the γ-part of the T(5) model, $\sin(3\gamma)$ in Eq. (7) is approximately replaced by $\sin(3\gamma_e)$ for simplicity since we consider the harmonic oscillator potential having a minimum at $\gamma=\gamma_e$ [4] and the system behaving a small-amplitude oscillations around the equilibrium point γ_e. Then, Eq. (7) can approximately be rewritten as

$$[-\frac{1}{\langle\beta^2\rangle}\frac{\partial^2}{\partial\gamma^2}+\frac{1}{2}c(\gamma-\gamma_e)^2]\phi(\gamma)=\epsilon_\gamma\phi(\gamma) \tag{26}$$

with $c=2BC/\hbar^2$. By taking $\tilde{\gamma}=\gamma-\gamma_e$ [4], the above equation can be further transformed into the form

$$[-\frac{\partial^2}{\partial\tilde{\gamma}^2}+\frac{1}{2}c\langle\beta^2\rangle\tilde{\gamma}^2]\phi(\tilde{\gamma})=\epsilon_{\tilde{\gamma}}\langle\beta^2\rangle\phi(\tilde{\gamma}), \tag{27}$$

which is very similar to the corresponding equation in the Z(5) CPS [4] except for that the potential here is taken as $u(\gamma)\propto(\gamma-\gamma_e)^2$. Then the energy eigenvalues and eigenfunctions are shown as [4]

$$\epsilon_{\tilde{\gamma}}=\sqrt{\frac{2c}{\langle\beta^2\rangle}}(n_{\tilde{\gamma}}+\frac{1}{2}),\quad n_{\tilde{\gamma}}=0,1,2,\ldots \tag{28}$$

and

$$\phi_{n_{\tilde{\gamma}}}(\tilde{\gamma})=N_{n_{\tilde{\gamma}}}H_{n_{\tilde{\gamma}}}(b\tilde{\gamma})e^{-b^2\tilde{\gamma}^2/2} \tag{29}$$

with

$$b=(\frac{c\langle\beta^2\rangle}{2})^{1/4}, \tag{30}$$

where the normalization constant is given as

$$N_{n_{\tilde{\gamma}}}=\sqrt{\frac{b}{\sqrt{\pi}2^{n_{\tilde{\gamma}}}n_{\tilde{\gamma}}!}}. \tag{31}$$

One thus obtains the general expression of the total energy

$$E(\xi,s,L,n_{\tilde{\gamma}})=E_0+A'(x_{\xi,L})^2+B'n_{\tilde{\gamma}}, \tag{32}$$

where E_0, A', and B' are the corresponding parameters [4].

$B(E2)$ transition rates can be calculated by taking the quadrupole operator

$$T_u^{E2}=t\beta[D_{u,0}^{(2)}(\theta_i)\cos(\gamma)+\frac{1}{\sqrt{2}}(D_{u,2}^{(2)}(\theta_i)+D_{u,-2}^{(2)}(\theta_i))\sin(\gamma)], \tag{33}$$

where t is a scale factor. Specifically, $B(E2)$ transition rates are given as

$$B(E2;\,L_{i_{\xi_i s_i}}\to L_{f_{\xi_f s_f}})=\frac{|\langle\xi_f L_f s_f\parallel T^{E2}\parallel\xi_i L_i s_i\rangle|^2}{2L_i+1}. \tag{34}$$

In the calculation of reduced matrix elements in (34), the same approximation used for the Hamiltonian, $\gamma\approx\gamma_e$, is also used for the quadrupole operator defined in (33) [2]. Then the integral over $\tilde{\gamma}$ only contributes $\delta_{n_{\tilde{\gamma}_i}n_{\tilde{\gamma}_f}}$ due to the orthonormality of $\phi_{n_{\tilde{\gamma}}}(\tilde{\gamma})$ [4], which indicates that the $E2$ transitional rate calculated in the present scheme will not be affected by the form of $\phi(\gamma)$ no matter $\phi(\gamma)$ is directly solved from (7) or after some approximations solved from (26). The integral over β takes the form

$$I_\beta(\xi_i,s_i,L_i;\,\xi_f,s_f,L_f)=\int\beta\eta_{\xi_i,s_i,Li}(\beta)\eta_{\xi_f,s_f,Lf}(\beta)\beta^4d\beta, \tag{35}$$

while the integral over the Euler angles θ_i can be obtained by using the formula involving three Wigner functions [30]. The final result is given as

$$\begin{aligned}B(E2;\,&L_{i_{\xi_i s_i}}\to L_{f_{\xi_f s_f}})\\&=t^2I_\beta^2(\xi_i,s_i,L_i;\,\xi_f,s_f,L_f)\\&\times\Big\{\sum_{K_i,K_f}\sqrt{\frac{1}{(1+\delta_{K_i0})(1+\delta_{K_f0})}}\\&\times C_{s_iK_i}^{L_i}C_{s_fK_f}^{L_f}[\cos(\gamma_e)\langle 20L_iK_i|L_fK_f\rangle\delta_{K_iK_f}\\&+\frac{1}{\sqrt{2}}\sin(\gamma_e)\langle 2-2L_iK_i|L_fK_f\rangle\delta_{K_iK_f+2}\\&+\frac{1}{\sqrt{2}}\sin(\gamma_e)\langle 22L_iK_i|L_fK_f\rangle\delta_{K_iK_f-2}]\Big\}^2.\end{aligned} \tag{36}$$

Since the rotational function $\varphi_{M,s}^L(\theta_i)$ with $L=0,2,3,5$ defined in (10) can be analytically solved from (9) [29], one can get some analytical expressions of $B(E2)$ values, such as

$$\begin{aligned}B(E2;\,2_{\xi_i1}\to 0_{\xi_f1})&=\frac{t^2}{5}I_\beta^2(\xi_i,1,2;\,\xi_f,1,0)\cos^2(\gamma_e+\Gamma_e),\\B(E2;\,2_{\xi_i2}\to 0_{\xi_f1})&=\frac{t^2}{5}I_\beta^2(\xi_i,2,2;\,\xi_f,1,0)\sin^2(\gamma_e+\Gamma_e),\\B(E2;\,2_{\xi_i2}\to 2_{\xi_f1})&=\frac{2t^2}{7}I_\beta^2(\xi_i,2,2;\,\xi_f,1,2)\sin^2(\gamma_e-2\Gamma_e),\\B(E2;\,3_{\xi_i1}\to 2_{\xi_f1})&=\frac{5t^2}{14}I_\beta^2(\xi_i,1,3;\,\xi_f,1,2)\sin^2(\gamma_e+\Gamma_e),\\B(E2;\,3_{\xi_i1}\to 2_{\xi_f2})&=\frac{5t^2}{14}I_\beta^2(\xi_i,1,3;\,\xi_f,2,2)\cos^2(\gamma_e+\Gamma_e),\\B(E2;\,5_{\xi_i1}\to 3_{\xi_f1})&=\frac{21t^2}{110}I_\beta^2(\xi_i,1,5;\,\xi_f,1,3)\cos^2(\gamma_e+\Gamma_e),\\B(E2;\,5_{\xi_i2}\to 3_{\xi_f1})&=\frac{21t^2}{110}I_\beta^2(\xi_i,2,5;\,\xi_f,1,3)\sin^2(\gamma_e+\Gamma_e)\end{aligned} \tag{37}$$

with [29]

$$\Gamma_e=-\frac{1}{2}\arccos\Big(\frac{\cos(4\gamma_e)+2\cos(2\gamma_e)}{\sqrt{9-8\sin^2(3\gamma_e)}}\Big). \tag{38}$$

It is clear that the results for the ground band and γ band are given as those with $\xi=1$ and $n_{\tilde{\gamma}}=0$, while the results for the β band are those with $\xi=2$ and $n_{\tilde{\gamma}}=0$. In the following, we will only consider the low-lying states in the bands with $n_{\tilde{\gamma}}=0$.

3. Numerical examination

As mentioned previously, the T(5) CPS provides a possible dynamical connection between the X(5) and Z(5) CPSs. To demonstrate the connection, some typical energy ratios and $B(E2)$ ratios in the related models are listed in Table 1. As shown in Table 1, the T(5) results in the $\gamma_e=0°$ and $\gamma_e=30°$ limits correspond exactly to those of the X(5) and Z(5) CPSs, respectively. Specifically, the ratios E_{L_1}/E_{2_1} and E_{L_β}/E_{2_1} in the T(5) model decrease monotonously from the X(5) limit ($\gamma_e=0°$) to the Z(5) limit ($\gamma_e=30°$). In addition, it is shown in Table 1 that approximate degeneracy of 6_1 and 0_2 level appears in the T(5) model for all γ_e values indicating that the approximate degeneracy may be regarded as a signal of the T(5) CPS.

Table 1
Typical energy ratios and $B(E2)$ ratios for the ground band and β band calculated in the T(5) model with different γ_e compared with the corresponding quantities in X(5) and Z(5) CPSs [2,4].

	X(5)	T(5)							Z(5)
		$\gamma_e = 0°$	$\gamma_e = 5°$	$\gamma_e = 10°$	$\gamma_e = 15°$	$\gamma_e = 20°$	$\gamma_e = 25°$	$\gamma_e = 30°$	
E_{4_1}/E_{2_1}	2.90	2.90	2.90	2.89	2.83	2.71	2.48	2.35	2.35
E_{6_1}/E_{2_1}	5.43	5.43	5.42	5.37	5.17	4.73	4.22	3.98	3.98
E_{8_1}/E_{2_1}	8.48	8.48	8.47	8.33	7.86	7.03	6.24	5.88	5.88
E_{6_1}/E_{0_2}	0.96	0.96	0.97	1.00	1.04	1.04	1.02	1.02	1.02
E_{8_1}/E_{0_2}	1.50	1.50	1.52	1.56	1.58	1.54	1.51	1.50	1.50
E_{0_2}/E_{2_1}	5.65	5.65	5.57	5.34	4.99	4.55	4.12	3.91	3.91
E_{2_β}/E_{2_1}	7.45	7.45	7.37	7.27	6.78	6.34	5.91	5.70	5.70
E_{4_β}/E_{2_1}	10.69	10.69	10.60	10.59	9.89	9.22	8.40	7.96	7.96
$\frac{B(E2;\,4_1\to2_1)}{B(E2;\,2_1\to0_1)}$	1.60	1.60	1.60	1.61	1.64	1.67	1.63	1.59	1.59
$\frac{B(E2;\,6_1\to4_1)}{B(E2;\,2_1\to0_1)}$	1.98	1.98	1.99	2.02	2.10	2.22	2.27	2.20	2.20
$\frac{B(E2;\,8_1\to6_1)}{B(E2;\,2_1\to0_1)}$	2.28	2.28	2.28	2.34	2.50	2.71	2.73	2.64	2.64
$\frac{B(E2;\,0_2\to2_1)}{B(E2;\,2_1\to0_1)}$	0.62	0.62	0.63	0.64	0.66	0.69	0.73	0.75	0.75
$\frac{B(E2;\,2_\beta\to0_2)}{B(E2;\,2_1\to0_1)}$	0.80	0.80	0.79	0.79	0.79	0.78	0.78	0.77	0.77
$\frac{B(E2;\,4_\beta\to2_2)}{B(E2;\,2_1\to0_1)}$	1.20	1.20	1.20	1.19	1.22	1.24	1.22	1.19	1.19

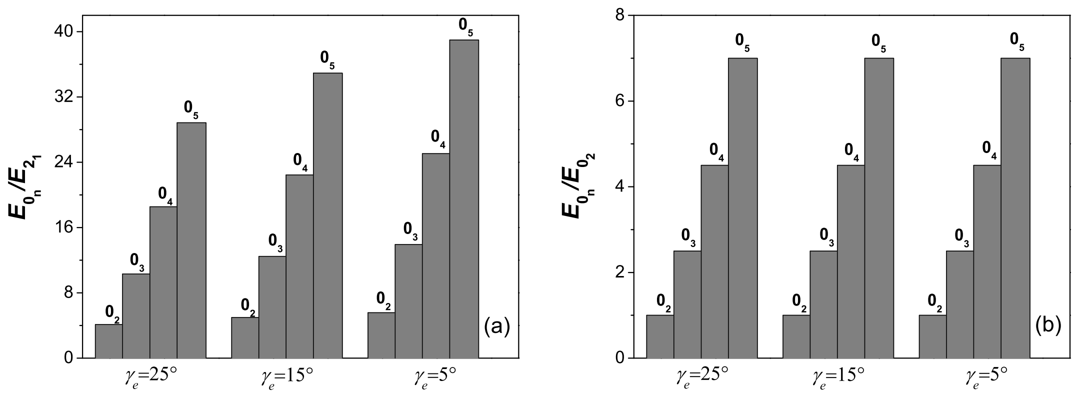

Fig. 1. The energy ratios E_{0_n}/E_{2_1} and E_{0_n}/E_{0_2} with n = 2, 3, 4, 5 calculated from the T(5) model for $\gamma_e = 5°, 15°, 25°$.

On the other hand, the analysis shown in [31,32] indicates that all 0^+ bandhead energies, E_{0_n}, in the CPS models should obey a universal law. However, it can be observed from Table 1 that the ratio E_{0_2}/E_{2_1} decreases with the increasing of γ_e. As a further analysis, the ratios E_{0_n}/E_{2_1} and E_{0_n}/E_{0_2} calculated from the T(5) CPS with several typical γ_e values are shown in Fig. 1. As shown in panel (a) of Fig. 1, the bandhead energies E_{0_n} with n = 2, 3, 4, 5 all monotonically increase with the decreasing of γ_e if they are normalized to E_{2_1}. However, if these bandhead energies are normalized to E_{0_2} as shown in panel (b), they all keep to be a constant independent of γ_e, which indeed coincide with the rule [31,32]

$$E_{0_n} = A(\mathrm{n}-1)(\mathrm{n}+2), \tag{39}$$

where A is an overall scale factor independent of γ_e. In fact, one can deduce from (15) and (22) that the bandhead energies E_{0_n} are only determined from Eq. (21) with $v = 3/2$, which is independent of the γ_e value in contrast to excited energies E_{L_n} with $L \neq 0$. It thus explains why the bandhead energies, E_{0_n}, obey the same law independent of γ_e.

Since the X(5) and Z(5) CPSs can be realized within the T(5) model in the $\gamma_e = 0°$ and $\gamma_e = 30°$ limit, respectively, it is expected that the T(5) model may play a role of the CPS for the transition from the spherical to triaxial deformation within $0° \le \gamma \le 30°$ (or equivalently the CPS of the transition from the spherical vibrator to a triaxial rotor). To elucidate this point, we compare level energies and the intraband B(E2) values in the ground band of the T(5) model with those obtained from the vibrator and the triaxial rotor at typical γ_e values. The results are shown in Fig. 2, in which the vibrator results are obtained from the U(5) limit (vibrational limit) of the interacting boson model [21], which is generally considered as an algebraic vibrator, while those of the triaxial rotor are obtained from the Davydov–Fillipov rotor model [28], of which the Hamiltonian is proportional to R_L defined in (5) [26]. It can be clearly seen from Fig. 2 that the results obtained from the T(5) model all fall in between those from the vibrator and the triaxial rotor with any γ deformation, which indicates that the T(5) model is indeed qualified to be regarded as the CPS of the shape phase transition from the vibrator to the triaxial rotor.

In order to check the sensitiveness of the T(5) model on γ_e further, several typical quantities as functions of γ_e are calculated, which are shown in Fig. 3. It can be observed in Fig. 3 that the T(5) model generally produces lower energy ratios and larger $B(E2)$ ratios in comparison to the corresponding results of the rigid triaxial rotor model. It is thus confirmed that the T(5) model may behave as a soft triaxial rotor [27]. Particularly, the $B(E2)$ ratio $B(E2: 3_\gamma \to 2_\gamma)/B(E2;\, 2_1 \to 0_1)$ in the rotor model remains to be a constant independent of γ_e, while this quantity in the T(5) model decreases monotonically as a function of γ_e. In addition, it is shown that the energy ratio E_{2_γ}/E_{2_1} may be taken as an indicator of γ_e value for the T(5) CPS because this quantity is very sensitive to γ_e, which is also relatively easily to be measured. Once γ_e is fixed by fitting the experimental energy ratio E_{2_γ}/E_{2_1}, the whole spectral structure is determined by the model up to an overall scale factor. It should be emphasized that all the energy ratios and $B(E2)$ ratios in the T(5) model shown in Fig. 3 at $\gamma_e = 30°$

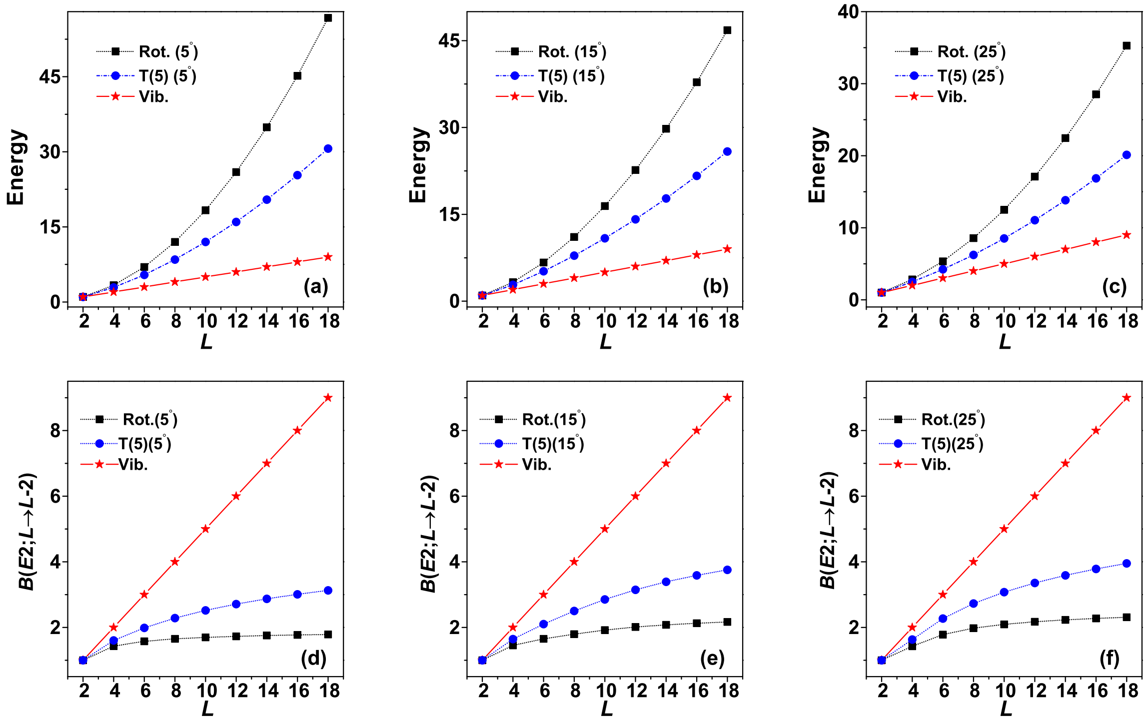

Fig. 2. (Color online.) The excited energies and $B(E2)$ values in the ground band calculated from the T(5) model (T(5)), those of the vibrational limit of the interacting boson model (Vib.) and those of the rotor model (Rot.) at $\gamma_e = 5°, 15°, 25°$, respectively, where the excited energies have been normalized to E_{2_1}, and the B(E2) values are normalized to $B(E2;\, 2_1 \to 0_1)$.

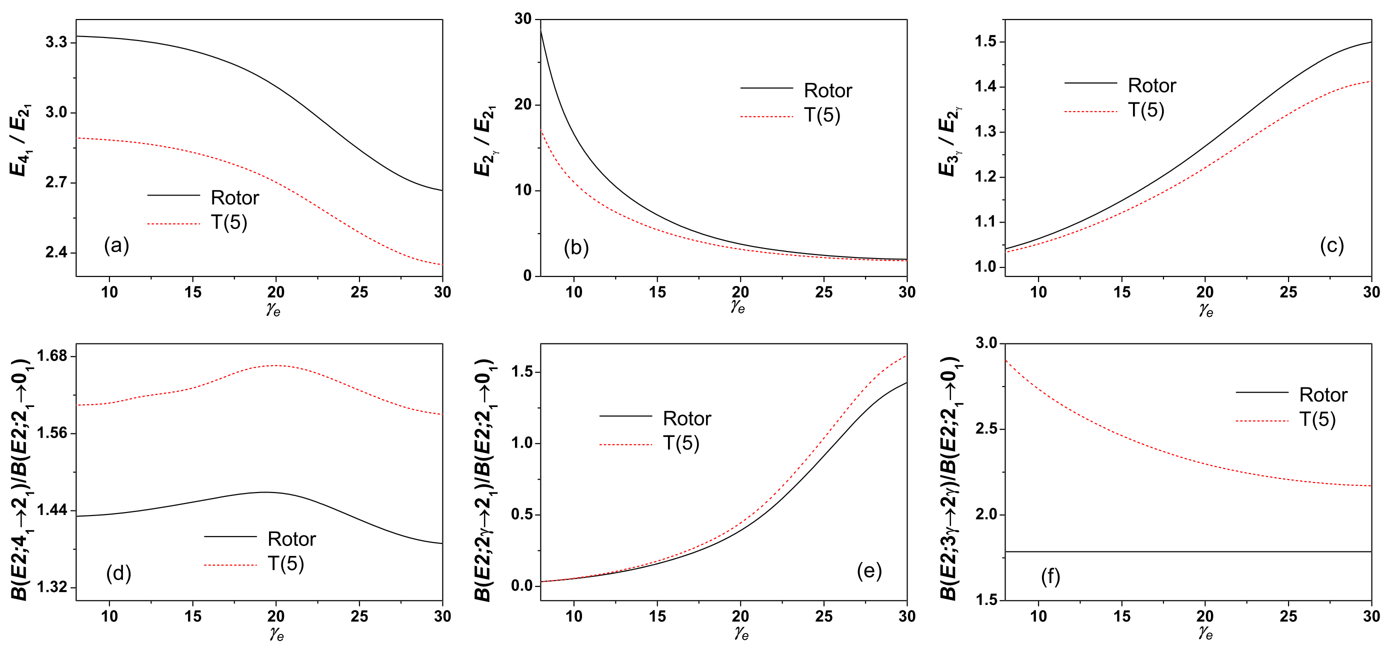

Fig. 3. (Color online.) Typical energy ratios and $B(E2)$ ratios calculated from the T(5) model and the rigid rotor model (the Davydov–Fillipov rotor [28]) as functions of γ_e.

coincide with those in the Z(5) CPS [4]. However, the quantities related to the γ band in the X(5) CPS cannot be derived from the present T(5) description in the $\gamma_e = 0°$ limit. For example, the ratio E_{2_γ}/E_{2_1} tends to infinity in the T(5) model as $\gamma \to 0°$, while it is a harmonic strength-dependent quantity in the X(5) model [2, 27]. In order to reproduce the X(5)-like γ band in the T(5) model at $\gamma_e = 0°$, one has to regroup the quantities in (6) and (7) by absorbing the term $\frac{K^2}{\sin^2(\gamma_e)|_{\gamma_e \to 0°}}$ into (7) as mentioned previously, which will be further explored in our future work.

4. Comparison to experiment

As shown in previous section, the T(5) model may provide a dynamical connection between the X(5) CPS [2] and Z(5) CPS [4], which thus offers a more flexible description of nuclei in between the two CPSs, such as either those supposed to be the candidates of the X(5) CPS with the neutron number $N = 90$ [33], or the candidates of the Z(5) CPS in the Pt isotopic chain [4]. To test the validity of the model, ^{148}Ce [34], ^{160}Yb [35], ^{192}Pt [36] and ^{194}Pt [37]

Table 2
Typical energy ratios and $B(E2)$ ratios for ^{148}Ce [34], ^{160}Yb [35], ^{192}Pt [36] and ^{194}Pt [37], and those calculated from the T(5) model with the γ_e value fitted to the ratio E_{2_γ}/E_{2_1}, where "−" denotes the corresponding quantity is not determined experimentally.

	(γ_e, nuclei)			
	(13°, ^{148}Ce)	(19°, ^{160}Yb)	(26°, ^{192}Pt)	(28°, ^{194}Pt)
E_{4_1}/E_{2_1}	(2.86, 2.86)	(2.74, 2.63)	(2.44, 2.48)	(2.37, 2.47)
E_{6_1}/E_{2_1}	(5.27, 5.30)	(4.84, 4.72)	(4.14, 4.31)	(4.03, 4.30)
E_{8_1}/E_{2_1}	(8.11, 8.14)	(7.20, 7.14)	(6.12, 6.38)	(5.94, 6.04)
E_{10_1}/E_{2_1}	(11.29, 11.31)	(9.85, 9.76)	(8.34, 7.96)	(8.11, −)
E_{6_1}/E_{0_2}	(1.03, 1.09)	(1.04, 1.06)	(1.02, 1.14)	(1.02, 1.11)
E_{2_γ}/E_{2_1}	(6.78, 6.25)	(3.46, 3.37)	(2.04, 1.94)	(1.89, 1.89)
E_{3_γ}/E_{2_1}	(7.38, 7.05)	(4.58, 4.14)	(2.79, 2.91)	(2.64, 2.81)
E_{4_γ}/E_{2_1}	(8.19, 7.72)	(5.16, −)	(4.32, 3.80)	(4.36, 3.74)
E_{5_γ}/E_{2_1}	(9.12, 8.98)	(6.06, −)	(4.81, 4.68)	(4.68, 4.56)
$\frac{B(E2;\,4_1\to 2_1)}{B(E2;\,2_1\to 0_1)}$	(1.63, −)	(1.67, 1.39)	(1.62, 1.56)	(1.60, 1.72)
$\frac{B(E2;\,6_1\to 4_1)}{B(E2;\,2_1\to 0_1)}$	(2.06, −)	(2.20, 1.80)	(2.26, 1.23)	(2.22, 1.36)
$\frac{B(E2;\,2_\gamma\to 0_1)}{B(E2;\,2_1\to 0_1)}$	(0.04, −)	(0.07, −)	(0.03, 0.01)	(0.01, 0.01)
$\frac{B(E2;\,2_\gamma\to 2_1)}{B(E2;\,2_1\to 0_1)}$	(0.11, −)	(0.36, −)	(1.19, 1.91)	(1.49, 1.81)
$\frac{B(E2;\,3_\gamma\to 2_\gamma)}{B(E2;\,2_1\to 0_1)}$	(2.55, −)	(2.32, −)	(2.19, 1.77)	(2.18, −)
$\frac{B(E2;\,4_\gamma\to 4_1)}{B(E2;\,2_1\to 0_1)}$	(0.15, −)	(0.39, −)	(0.39, −)	(0.35, 0.41)
$\frac{B(E2;\,4_\gamma\to 2_\gamma)}{B(E2;\,2_1\to 0_1)}$	(0.84, −)	(0.70, −)	(0.57, −)	(0.63, 0.45)

are chosen as candidates of the T(5) model. Notably, the γ_e value for each nucleus is obtained by fitting the experimental energy ratio E_{2_γ}/E_{2_1} since this ratio is very sensitive to γ_e as discussed previously. Then the spectral structure of the T(5) model is thus fixed up to a scale factor for each nucleus. Specifically, some typical energy ratios and $B(E2)$ ratios calculated from the T(5) model for these nuclei are listed in Table 2, which are compared with the corresponding experimental data. It is clearly shown in Table 2 that the results of each nucleus are well reproduced in the T(5) model with the γ_e value fitted to the experimental energy ratio E_{2_γ}/E_{2_1}. Particularly, while the ratio E_{2_γ}/E_{2_1} changes noticeably as a function of γ_e from nucleus to nucleus, the ratio $E_{6_1}/E_{0_2}\sim 1$ indeed keeps almost unchanged as predicted in the T(5) model. In addition, it can also be observed that the ideal value of γ_e in the T(5) model for ^{192}Pt and ^{194}Pt is very close to 30°, which indicates that the original Z(5) description of these nuclei [4] is robust. Anyway, it seems that the T(5) model with the γ_e parameter fitted to the energy ratio E_{2_γ}/E_{2_1} indeed provides a reasonable description for these transitional nuclei.

5. Summary

In summary, the critical point symmetry, called T(5), has been introduced by approximately separating variables in the Bohr Hamiltonian for any given γ value. It was shown that the T(5) model provides a dynamical connection between the original X(5) and Z(5) CPSs [2,4], of which the two CPSs just correspond to the limiting cases of the T(5) model. It was also shown that the model provides a better description of the spectral patterns of ^{148}Ce, ^{160}Yb, ^{192}Pt, and ^{194}Pt, which in turn indicates that possible triaxial deformation may be involved to some extent in these transitional nuclei. In addition, it is shown that the T(5) model provides the energy and the B(E2) ratios in between those of the vibrator and the rigid triaxial rotor, indicating that the model may also serve as the CPS description for the spherical to the triaxial deformed shape phase transition [12,21].

Finally, our recent work has shown that the E(5) and X(5) CPSs dynamics may be algebraically realized with the Euclidean dynamical symmetry [38,39]. It should be interesting to see whether the T(5) model description can also be unified in the Euclidean dynamical symmetry description by using similar algebraic technique. On the other hand, based on the successful CPS descriptions in even–even system, the CPS concept was also extended to odd–A systems [40–46]. However, these extensions of the CPSs are mostly focused on the axially symmetric situation. The T(5) model description may provide a new starting point to establish the CPS description for the triaxial deformation in the transitional odd–A nuclei. On the other hand, new methods have been developed to obtain accurate numerical solutions for a diverse range of collective Hamiltonians [47–51], from which the validity of the approximate separation of variables introduced with the X(5) CPS has been examined by Caprio [52]. It should also be possible and necessary to further check the validity of the present approximate solutions of the T(5) model in a similar way [52]. Related work in this direction is in progress.

Acknowledgements

Support from U.S. National Science Foundation (OCI-0904874), Southeastern Universities Research Association, the Natural Science Foundation of China (11375005, 11005056, 11175078, 11375080, and 11475091), and the LSU–LNNU joint research program (9961) is acknowledged.

References

[1] F. Iachello, Phys. Rev. Lett. 85 (2000) 3580.
[2] F. Iachello, Phys. Rev. Lett. 87 (2001) 052502.
[3] F. Iachello, Phys. Rev. Lett. 91 (2003) 132502.
[4] D. Bonatsos, D. Lenis, D. Petrellis, P.A. Terziev, Phys. Lett. B 588 (2004) 172.
[5] D. Bonatsos, D. Lenis, D. Petrellis, P.A. Terziev, I. Yigitoglu, Phys. Lett. B 621 (2005) 102;
D. Bonatsos, D. Lenis, D. Petrellis, P.A. Terziev, I. Yigitoglu, Phys. Lett. B 632 (2006) 238.
[6] D. Bonatsos, D. Lenis, N. Minkov, D. Petrellis, P.P. Raychev, P.A. Terziev, Phys. Rev. C 70 (2004) 024305.
[7] M. Caprio, Phys. Rev. C 65 (2002) 031304(R).
[8] M. Caprio, Phys. Rev. C 69 (2004) 044307.
[9] L. Fortunato, Phys. Rev. C 70 (2004) 011302(R).
[10] N. Pietralla, O.M. Gorbachenko, Phys. Rev. C 70 (2004) 011304(R).
[11] R.F. Casten, E.A. McCutchan, J. Phys. G 34 (2007) R285.
[12] P. Cejnar, J. Jolie, R.F. Casten, Rev. Mod. Phys. 82 (2010) 2155.
[13] R.F. Casten, N.V. Zamfir, Phys. Rev. Lett. 85 (2000) 3584;
R.F. Casten, N.V. Zamfir, Phys. Rev. Lett. 87 (2001) 052503.
[14] R.M. Clark, et al., Phys. Rev. C 68 (2003) 037301;
R.M. Clark, et al., Phys. Rev. C 69 (2004) 064322.
[15] D.L. Zhang, Y.X. Liu, Phys. Rev. C 65 (2002) 057301.
[16] A. Frank, C.E. Alonso, J.M. Arias, Phys. Rev. C 65 (2001) 014301.
[17] N.V. Zamfir, et al., Phys. Rev. C 65 (2002) 044325.
[18] C. Mihai, et al., Phys. Rev. C 75 (2007) 044302.
[19] J.F. Zhang, et al., Chin. Phys. Lett. 20 (2003) 1231.
[20] L. Coquard, et al., Phys. Rev. C 80 (2009) 061304(R).
[21] F. Iachello, A. Arima, The Interacting Boson Model, Cambridge University, Cambridge, England, 1987.
[22] P. Van Isacker, J.Q. Chen, Phys. Rev. C 24 (1981) 684.
[23] L. Fortunato, C.E. Alonso, J.M. Arias, J.E. Garìa-Ramos, A. Vitturi, Phys. Rev. C 84 (2011) 014326.
[24] Y.F. Smirnov, N.A. Smirnova, P. Van Isacker, Phys. Rev. C 61 (2000) 041302(R).
[25] Y. Zhang, F. Pan, L.R. Dai, J.P. Draayer, Phys. Rev. C 90 (2014) 044310.
[26] A. Bohr, Mat.-Fys. Medd. Danske Vid. Selsk. 26 (14) (1952).
[27] R. Bijker, R.F. Casten, N.V. Zamfir, E.A. McCutchan, Phys. Rev. C 68 (2003) 064304.
[28] A.S. Davydov, G.F. Fillipov, Nucl. Phys. 8 (1958) 237.
[29] J.L. Wood, A.M. Oros-Peusquens, R. Zaballa, J.M. Allmond, W.D. Kulp, Phys. Rev. C 70 (2004) 024308;
J.M. Allmond, Ph.D. dissertation, Georia Institute of Technology, 2007, http://hdl.handle.net/1853/14604.
[30] A.R. Edmonds, Angular Momentum in Quantum Mechanics, Princeton Univ. Press, Princeton, 1957.
[31] D. Bonatsos, E.A. McCutchan, R.F. Casten, Phys. Rev. Lett. 101 (2008) 022501.
[32] D. Bonatsos, E.A. McCutchan, R.F. Casten, R.J. Casperson, V. Werner, E. Williams, Phys. Rev. C 80 (2009) 034311.
[33] R.F. Casten, Nat. Phys. 2 (2006) 811.
[34] M.R. Bhat, Nucl. Data Sheets 89 (2000) 797.

[35] C.W. Reich, Nucl. Data Sheets 105 (2006) 557.
[36] C.M. Baglin, Nucl. Data Sheets 84 (1998) 717.
[37] E. Browne, B. Singh, Nucl. Data Sheets 79 (1996) 277.
[38] Y. Zhang, Y.X. Liu, F. Pan, Y. Sun, J.P. Draayer, Phys. Lett. B 732 (2014) 55.
[39] Y. Zhang, F. Pan, Y.X. Liu, Y.A. Luo, J.P. Draayer, Phys. Rev. C 90 (2014) 064318.
[40] F. Iachello, Phys. Rev. Lett. 95 (2005) 052503.
[41] C.E. Alonso, J.M. Arias, A. Vitturi, Phys. Rev. Lett. 98 (2007) 052501.
[42] C.E. Alonso, J.M. Arias, A. Vitturi, Phys. Rev. C 75 (2007) 064316.
[43] Y. Zhang, F. Pan, Y.X. Liu, Z.F. Hou, J.P. Draayer, Phys. Rev. C 82 (2010) 034327.
[44] Y. Zhang, F. Pan, Y.X. Liu, Y.A. Luo, J.P. Draayer, Phys. Rev. C 84 (2011) 034306.
[45] Y. Zhang, F. Pan, Y.X. Liu, J.P. Draayer, Phys. Rev. C 84 (2011) 054319.
[46] Y. Zhang, F. Pan, Y.A. Luo, Y.X. Liu, J.P. Draayer, Phys. Rev. C 86 (2012) 044312.
[47] D.J. Rowe, Nucl. Phys. A 735 (2004) 372.
[48] D.J. Rowe, P.S. Turner, J. Repka, J. Math. Phys. 45 (2004) 2761.
[49] D.J. Rowe, P.S. Turner, Nucl. Phys. A 753 (2005) 94.
[50] D.J. Rowe, T.A. Welsh, M.A. Caprio, Phys. Rev. C 79 (2009) 054304.
[51] G. Thiamova, D.J. Rowe, M.A. Caprio, Nucl. Phys. A 895 (2012) 20.
[52] M.A. Caprio, Phys. Rev. C 72 (2005) 054323.